Chain Anisotropy of Side-Group Liquid Crystalline Polymers in Nematic Solvents

Michael D. Kempe,[†] Julia A. Kornfield,*[,†] and Jyotsana Lal[‡]

Division of Chemistry and Chemical Engineering, 210-41, California Institute of Technology, Pasadena, California 91125, and Argonne National Laboratory, Argonne, Illinois 60439

Received June 17, 2003; Revised Manuscript Received August 20, 2004

ABSTRACT: We demonstrate a method for measuring the anisotropy of a side group liquid crystalline polymer (SGLCP) in a perdeuterated nematic solvent using small-angle neutron scattering. In this system scattering originates from both the polymer backbone and the large pendant side groups, causing the measured anisotropy to vary with molecular weight. Since it is the backbone anisotropy that is of interest, we show how to mathematically account for scattering due to the side groups. Using a molecular weight series of SGLCPs that have an oblate conformation, this method yields a constant ratio of the backbone radii independent of molecular weight and spacer length.

1. Introduction

When a polymer is dissolved in a nematic host, it adopts an anisotropic conformation that is coupled to the nematic order of the liquid crystal, giving rise to rheologically complex behavior. The Brochard[1] theory predicts that the addition of a polymer with an oblate (or disklike) spheroid conformation to a flow aligning nematic host will result in a material where the director tumbles in response to an imposed shear. In contrast, this theory also predicted that the addition of a polymer with a prolate spheroid conformation would increase the tendency of the director to flow align at a steady-state angle near the velocity direction. The Brochard theory also describes how, in a dilute solution, the anisotropy of the polymer affects the six Leslie−Erickson parameters used to describe the viscosity of a nematic material. Numerous rheological studies have been performed to test the qualitative validity of the Brochard theory[2,3] or to obtain estimates for the chain anisotropy.[4−7] In the work of Yao and Jamieson[7] electrorheological measurements of solutions of a side-group liquid crystalline polymer (SGLCP) in a nematic solvent were used to obtain estimates of the polymer chain anisotropy using the Brochard theory. They found that as the molecular weight is increased, the rheologically inferred anisotropy, $R_\perp/R_\parallel$, increases. Despite interest in the anisotropy of SGLCPs in nematic solutions, little research[8−10] has been performed to test the validity of the Brochard theory.

Two predominant types of chain conformations are found for SGLCPs: a prolate spheroid conformation with both the backbone and the mesogenic units aligned near the director and an oblate, or disklike, spheroid conformation with the backbone preferentially perpendicular to the director. Theoretical descriptions[11−14] of the sense of the anisotropy and its magnitude predict a molecular weight dependence for low molecular weight and a constant anisotropy at high molecular weight.

Although there are numerous theories and experiments designed to predict the dimensions of an SGLCP in a nematic solution, little work has been done to measure the anisotropy of a liquid crystal polymer in a small molecule nematic LC. In principle, the backbone anisotropy can be measured using small-angle neutron scattering[15] (SANS) or X-ray scattering.[2,16,17] In practice, the lack of data on polymers dissolved in nematic solvents reflects the difficulty of obtaining adequate scattering intensity to perform these experiments. Solution studies are performed with a relatively low concentration of about 5 wt % polymer, as opposed to a 50:50 deuterated/hydrogenated polymer mixture in melt studies. Furthermore, the effects of scattering from the bulky side chains are typically eliminated by only labeling the backbone (deuterium labeling in SANS or silicon atoms for SAXS). Unfortunately, this results in an order of magnitude lower effective concentration of scatterers.[18−20]

To maximize the contrast in neutron scattering experiments, it is possible to label either the entire polymer or solvent molecule with deuterium. The problem with these two approaches is that the effects of scattering on the mesogenic groups must be accounted for to determine the backbone conformation. Using an end-on SGLCP based on a poly(methylsiloxane) in which the terminal ends of the mesogenic units were labeled with deuterium, researchers[20−23] observed a prolate conformation. With the same polymer labeled on the spacer near the backbone, an oblate conformation was observed.[24] When scattering results from deuteration of the mesogenic units, a larger radius is measured parallel to the director.[20−24] Unless the polymer is large, this leads to an erroneous determination of the polymer anisotropy. Casquilho and Volino[25] suggested that the results of labeling on different parts of the mesogenic unit could be extrapolated to the case for labeling on the backbone only. Unfortunately, this method requires a series of differently labeled polymers making this method impractical. Therefore, a method to account for scattering on partially or fully labeled SGLCPs is needed.

In this work, we use the solvent labeling approach to eliminate the need for labeling the polymer and demonstrate a way to account for the scattering from the mesogenic units. The SANS pattern of a series of low-polydispersity polymers differing only in their molecular weight reveal an anisotropy that increases with molec-

[†] California Institute of Technology.
[‡] Argonne National Laboratory.

10.1021/ma034825f CCC: $27.50
Published on Web 10/22/2004

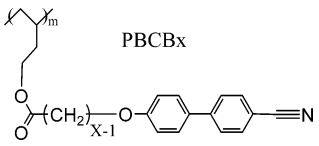

Figure 1. Structure for polymers used in this study. The "*X*" in the polymer name indicates the size of the spacer where $X + 4$ is the number of atoms between the mesogen and the polymer backbone.

ular weight. Once the scattering due to the mesogenic units is accounted for, the backbone anisotropy is found to be independent of molecular weight. In addition, the backbone anisotropy is found to be independent of spacer length in the side group over the range probed, $x = 4-8$ in Figure 1. By demonstrating a way to measure the polymer anisotropy in solution, we provide direct measurements of chain anisotropy. This is required to test the relationships between chain anisotropy and the effect of polymers on the flow behavior of nematic LCs.[26] In turn, the results will reveal the relationships between polymer structure, conformation, viscoelastic response, and electrooptic response.

2. Experimental Methods

2a. Materials. The details of the synthesis and characterization of the polymers used in this study are published elsewhere.[27] A series of SGLCPs differing in either the degree of polymerization (DP) or in the number of carbons in the spacer unit were produced by hydroboration/oxidation of 1,2-polybutadiene followed by attachment of a mesogenic side group using an acid chloride reaction (Figure 1). By matching the structure of the mesogen to the small molecule nematic LC, good solubility of these polymers was found in the liquid crystals 4′-pentyl-4-cyanobiphenyl (5CB) and 4′-pentyloxy-4-cyanobiphenyl (5OCB) and in the eutectic mixtures E7 and E44.[28] These polymers seem to be soluble in almost any nematic, cyanobiphenyl-based LC.

The refractive indices of solutions of 420 kg/mol PBCB6 in 5CB were measured using an Abbe refractometer. For up to 10 wt % polymer at temperatures at least 3 °C away from the nematic-to-isotropic transition temperature ($T \leq 32$ °C), the ordinary and extraordinary refractive indices of the solution were equal to those of 5CB. This indicates that added polymer does no change the order parameter of the nematic host over this range of concentrations.

2b. Size Exclusion Chromatography (SEC) and Multiangle Laser Light Scattering (MALLS). The radius of gyration of the PBCB6 polymers and of the 1,2-polybutadiene prepolymers were measured using multiangle laser light scattering (MALLS). Gel permeation chromatography (GPC) was carried out on two Polymer Labs 30 cm long PLgel 5 μm mixed-C columns (200−2 000 000 g/mol) connected in series with a DAWN EOS (MALLS) detector and an Optilab DSP differential refractometer both from Wyatt Technology. The MALLS detector used a 30 mW, 690 nm, gallium arsenide linearly polarized laser, and the differential refractometer used 690 nm light with a Wollaston prism. Tetrahydrofuran was used as the eluant at a flow rate of 1 mL/min and a temperature of 35 °C.

The molecular weight distribution was analyzed using the ASTRA software from Wyatt Technology Corp. The refractive index increment dn/dc of the polymer was determined assuming the polymer was completely eluted. A value for dn/dc of 0.16 mg/mL was obtained for the PBCBx series of polymers from an average of several runs.[27] In our experience, this method provided reproducible values of dn/dc to within ±0.005 mg/mL for chromatograms for which the baseline was well-defined before the polymer begins to elute and returns to that baseline following the elution peak. The Rayleigh ratio of the solution was measured at up to 18 angles at each point in the chromatogram. The radius of gyration was calculated using the Gunnier approximation to specify the angular dependence $P(\theta)$ in the Zimm expression

$$\frac{K^*c}{R(\theta,c)} = \frac{1}{M_w P(\theta)} + 2cA_2 \tag{1}$$

Here $K^* = 4\pi^2(\mathrm{d}n/\mathrm{d}c)^2 n_0^2/N_a\lambda_0^4$ and $R(\theta,c)$ is the excess Rayleigh ratio of the solution as a function of scattering angle θ and concentration c. $R(\theta,c)$ is directly proportional to the intensity of the scattered light in excess of the light scattered by the pure solvent. The concentration was kept low allowing the osmotic compressibility contribution (A_2) to be neglected. Thus, at each point in the chromatogram there was sufficient information to evaluate M_w. Similarly, the concentration was evaluated at each point in the chromatogram using dn/dc, which was used with the M_w of each fraction to calculate the PDI, M_n, and M_z of the polymer.

2c. Chain Conformation by Small-Angle Neutron Scattering. The radii of gyration of a series of PBCBx polymers were determined by neutron scattering using hydrogenated polymers in a perdeuterated solvent 4′-pentyl-4-cyanobiphenyl-d_{19} (D5CB). The D5CB was synthesized by exchanging the hydrogen in 4-pentylbiphenyl for deuterium using D_2O and a Pt catalyst, followed by attachment of a nitrile group. The resulting material had 95% of its hydrogen exchanged for deuterium and had properties similar to its hydrogenated analogue.[29] Solutions were prepared by mixing the polymer and D5CB in dichloromethane and removing the dichloromethane under vacuum. All solutions were made with 5 wt % polymer to keep them below the overlap concentration ($C^* \geq$ 20 wt % for all samples).

Neutron scattering experiments were conducted at the Intense Pulsed Neutron Source (IPNS) at Argonne National Laboratory using the small-angle diffraction (SAD) instrument. The samples were loaded into a cell made up of two 1 in. diameter $^1/_8$ in. thick quartz windows separated by a 0.5 mm spacer. Homogeneous (parallel) alignment of the sample was obtained by using both rubbed polyimide layers on the quartz windows and a 0.8 T magnetic field oriented in the rubbing direction. A small gap was used so that excellent alignment could be obtained and so the sample would not flow out of the cell. A cell containing bulk D5CB was used as a blank, and the scattering patterns were acquired for between 5 and 10 h at 25 °C.

2d. Data Reduction (SANS). The SANS patterns are anisotropic with elliptical isointensity contours with the major axis parallel to the director (Figure 2). Since a higher scattering intensity is measured parallel to the director and quadratic characteristic sizes parallel and perpendicular to the director, $R_{||}$ and $R_\perp$, are inversely related to the scattering intensity, this shows that $R_{||} < R_\perp$, which corresponds to an oblate conformation. Typically,[30] the values for the radii of gyration are found by analyzing a slice of the data both parallel and perpendicular to the director and fitting the low q data with a Guinier approximation to yield the quadratic characteristic size in a direction $\vec{x}$

$$\frac{I_0}{I(q)} = 1 + q^2 R_x^{\,2} + \ldots \tag{2}$$

The high molecular weight of our polymers resulted in fewer data points for the low q range ($qR_g < 1$); therefore, the scattering patterns were fit to the Debye equation

$$I(q) = I_0\left(\frac{2}{q^4 R_g^{\,4}}\right)[q^2 R_g^{\,2} - 1 + \mathrm{e}^{-q^2 R_g^{\,2}}] \tag{3}$$

so that the intermediate range ($1 < qR_g < 3$) could be used.[13,31,32]

We are concerned with determining the characteristic quadratic size, R_x, particularly where $\vec{x}$ is either parallel or

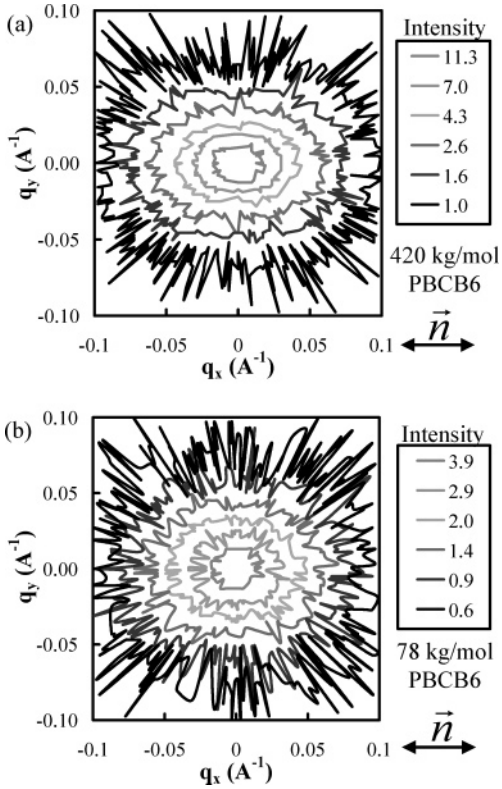

Figure 2. Contour intensity plot of the neutron scattering pattern for (a) 420 kg/mol PBCB6 and (b) 78 kg/mol PBCB6 dissolved in D5CB. In these plots, the director is oriented along the "*x*" direction.

perpendicular to the director. For an isotropic polymer the quadratic size is related to the radius of gyration by[33]

$$R_g = \sqrt{3}R_x \tag{4}$$

Since the Debye equation is used to determine R_g for an isotropic polymer, the radius determined from a fit of eq 3 is divided by $\sqrt{3}$ to yield $R_\perp$ or $R_\parallel$.

Since our polymers are in the dilute regime and the samples were thin, the scattering intensity is low. To overcome this problem, we use the entire scattering pattern in our analysis to improve the statistics.[34] To do this the radius is determined as a function of azimuthal angle (θ). In an anisotropic medium a polymer is often in the shape of either an oblate or a prolate spheroid; therefore, the isointensity contours were modeled using an ellipse

$$\left(\frac{1}{R_x(\theta)}\right)^2 = \left(\frac{\sin\theta}{R_\parallel}\right)^2 + \left(\frac{\cos\theta}{R_\perp}\right)^2 \tag{5}$$

with θ defined as the angle between q and the director ($\vec{n}$).[35]

Since each monomeric unit has a large, fully hydrogenous side group, the Debye equation can only be applied as an approximation. The Debye model describes the scattering from a connected set of freely jointed scatterers of which the shape and size are not accounted for. Only for values of $q \ll 1/L$, where L is the characteristic length of a side group, can the mesogen be approximated as a single scatterer.[36] Since our polymers are large, the relative contributions of the side groups to the measured radii are still small. Therefore, to a first-order approximation, the side group simply increases the effective R_g as measured in the Debye equation.[37]

Since the scattered intensity is a function of the product qR_x, the ratio of the quadratic characteristic sizes, $R_\perp/R_\parallel$, was determined by plotting $I(q)$ vs $q_\parallel$ and $I(q)$ vs $q_\perp R_\perp/R_\parallel$ and adjusting the ratio $R_\perp/R_\parallel$ until the profiles of the two plots

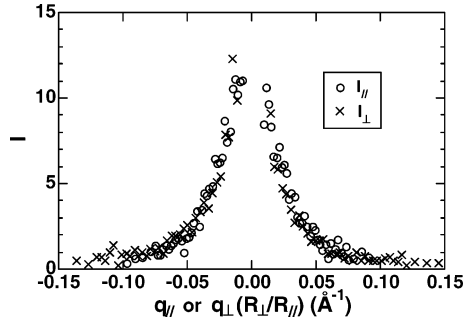

Figure 3. Representative plot used for the determination of the polymer anisotropy using data for 420 kg/mol PBCB6 in D5CB. The anisotropy ratio of $R_\perp/R_\parallel$ is adjusted until the two profiles superimpose as shown.

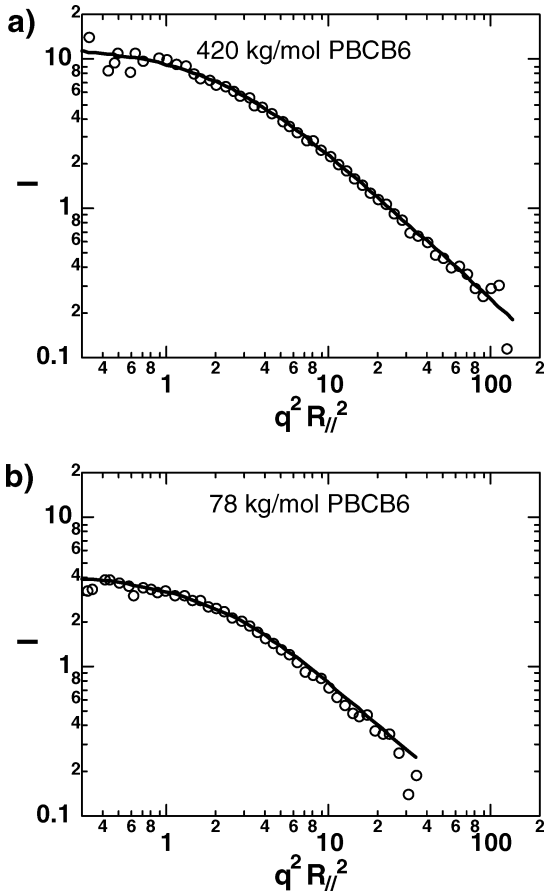

Figure 4. Plot of the Debye function used to determine values for the radii: (a) 420 kg/mol PBCB6 and (b) 78 kg/mol PBCB6 dissolved in D5CB.

matched with good overlap (Figure 3). The uncertainty reported for this ratio was determined by finding the maximum and minimum values for which the data could be reasonably interpreted.

Since there was a low signal-to-noise ratio in the measurement of the scattered intensity, data points that had similar values of $qR_x(\theta)$ were averaged prior to fitting with the Debye equation. With the ratio $R_\perp/R_\parallel$ known, the Debye equation was fit to the data by adjusting I_0 and $R_\parallel$ on a plot of $I(q)/I_0$ vs $R_x(\theta)^2q^2$ until a good fit to the data was found (Figure 4). To confirm the validity of the radii obtained, plots of $I(q)/I_0$ vs q containing data points parallel or perpendicular to the director were plotted along with the intensity calculated with the Debye equation using $R_\parallel$ or $R_\perp$, respectively (Figure 5). The uncertainty in the measured values of the radii was obtained by finding the maximum and minimum values for which the data could be fit.

Table 1. Neutron Scattering Results[a]

polymer sample	M_n (kg/mol)	$R_\perp$ (Å)	$R_\parallel$ (Å)	$R_\perp/R_\parallel$	$R_{\perp b}$ (Å)	$R_{\parallel b}$ (Å)	$R_{\perp b}/R_{\parallel b}$
PBCB4	388	64 ± 6	42 ± 4	1.52 ± 0.05	64 ± 6	41 ± 4	1.56 ± 0.05
PBCB5	404			1.52 ± 0.15			1.57 ± 0.15[b]
PBCB6	78	30 ± 4	21 ± 3	1.42 ± 0.05	30 ± 4	18 ± 3	1.64 ± 0.05
PBCB6	139	32 ± 4	22 ± 3	1.43 ± 0.05	31 ± 4	19 ± 3	1.62 ± 0.05
PBCB6	364	59 ± 7	37 ± 5	1.60 ± 0.05	59 ± 7	35 ± 5	1.69 ± 0.05
PBCB6	420	59 ± 6	37 ± 4	1.61 ± 0.06	59 ± 6	35 ± 4	1.68 ± 0.05
PBCB7	437	62 ± 6	41 ± 4	1.51 ± 0.05	62 ± 6	40 ± 4	1.56 ± 0.05
PBCB8	453			1.55 ± 0.1			1.61 ± 0.1[b]

[a] $R_\perp$ and $R_\parallel$ represent quadratic characteristic size of the polymer including the effects of the side groups, and $R_{\perp b}$ and $R_{\parallel b}$ represent the radii of the backbone only calculated using eqs 8 and 9. Molar masses are computed assuming 100% attachment of mesogen to the 1,2-polybutadiene prepolymer. Some of the data for the samples PBCB5 and PBCB8 were omitted since these polymers had high PDIs of ~1.9 and ~2.2, respectively. [b] This anisotropy was estimated based on $R_\perp = 61$ Å.

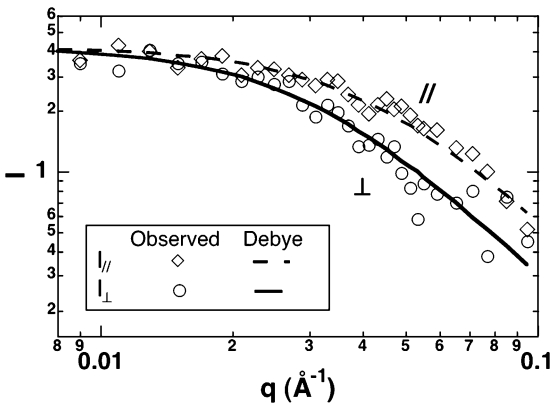

Figure 5. Plot of data points near the parallel and perpendicular directions used to confirm values for the radii. SANS for 5% 78 kg/mol PBCB6 in D5CB.

Table 2. MALLS Results

polymer sample	M_n[a] (kg/mol)	$R_x = R_g/\sqrt{3}$ (Å)	PDI	prepolymer R_x[b] (Å)
PBCB4	388	71 ± 20	1.16	81 ± 10
PBCB6	78		1.14	35 ± 10
PBCB6	364	73 ± 20	1.13	77 ± 10
PBCB6	420	107 ± 20	1.09	81 ± 10
PBCB7	437	126 ± 20	1.09	81 ± 10

[a] The molar masses listed in this table are those calculated based on 100% attachment of the mesogen to the backbone.[27] [b] Because of the large uncertainty in the measured radii of the 1,2-polybutadiene prepolymer the numbers listed are based on a fit to $R_x \propto \sqrt{M_w}$ from a set of eight polymer samples.

3. Results

SANS results were obtained for a molecular weight series of PBCB6 ranging from 78 up to 420 kg/mol (Table 1). The spacer length is also varied from 4 to 8 carbons, and the radii are reported for all but the samples PBCB8 and PBCB5.[27] For these two samples, unusually large values of R_x are linked to a high polydispersity resulting from cross-linking; therefore, these values are not reported.

In the isotropic THF solution the quadratic characteristic size (as determined by MALLS) of the SGLCP is greater than that of the prepolymer, and both are greater than either of the dimensions of the SGLCP in the nematic LC D5CB (Table 2). Comparison of the SGLCPs vs the corresponding 1,2-polybutadienes indicates that the addition of the side group increases the radii significantly. This increase is caused by decreased backbone flexibility and by the added bulk of the side group. It will be shown that, at the large molecular weights of our polymers, the additional contributions to the radii from the side groups are small; therefore, the increase in radii after attachment of the mesogen is primarily due to a decrease in the backbone flexibility.

4. Discussion

4a. Origin of Molecular Weight Dependent Anisotropy. The observed anisotropy of PBCB6 increases with chain length (Figure 2). A molecular weight dependence of the backbone anisotropy is not expected for the polymers in this molecular weight series which are all long enough so that their conformation can be described by a Gaussian distribution in a direction either parallel or perpendicular to the director. For very small molecular weights, i.e., oligomers, the backbone behaves more like a rod than a freely jointed chain. For a large polymer coil, the ratio of chain fluctuations parallel and perpendicular to the director should be independent of molecular weight and the anisotropy of the polymer should remain constant.[11−13]

O'Allest et al.[38] found a nematic main chain liquid crystal polymer, for which a constant backbone anisotropy was achieved for molecular masses above ~15 kg/mol. Similarly, Shibaev et al.[39] found the backbone anisotropy of a smectic polyacrylate SGLCP to increase until a molecular mass of approximately 100 kg/mol was achieved. They attributed the constant anisotropy to the ability of the long backbone to obtain a statistical number of layer crossings. Being free from smectic layering, our system would be expected to achieve constant backbone anisotropy at a much smaller molar mass than 100 kg/mol.

The explanation for the change in anisotropy in our SANS experiment is that the measured anisotropy combines contributions from the polymer backbone and the mesogenic units. In a nematic solution, the presence of ordered side groups contributes to the scattering pattern differently parallel and perpendicular to the director. In the case of an LC polymer composed of just a few monomers (Figure 6a), the prolate shape of the mesogenic groups can dominate.[20−22] As the molecular weight is increased, the backbone adopts an oblate conformation, which can counterbalance the mesogenic units that are preferentially parallel to the director, causing an overall spherical conformation (Figure 6b). Finally, at high molecular weights the overall polymer anisotropy is dominated by the backbone conformation (Figure 6c).

Similar effects of pendant side groups have also been reported by Rawiso et al.[36] for polystyrene that was isotopically selectively labeled on either the backbone or on the phenyl ring. To explain the anomalous SANS patterns that resulted, they approximated the polystyrene molecule as a curved cylinder and accounted for the scattering of the side groups as a distribution of

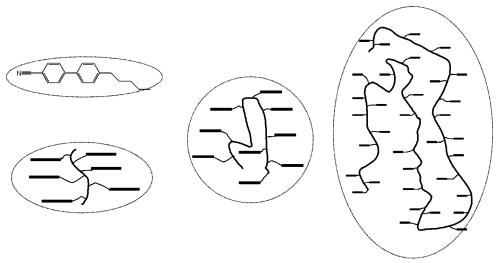

Figure 6. Schematic explanation of how the anisotropy of an oblate polymer can increase with increasing molecular weight. Rotation of these 2-D figures around the director will produce 3-D (a) prolate speroids, (b) spheres, or (c) oblate speroids.

Table 3. Calculation of PBCB6 Component Scattering Length Densities

component	M (g/mol)	ρ (g/cm^3)	δ 10^{10} (cm^{-2})	$K = (\delta_{D5CB} - \delta)$ 10^{10} (cm^{-2})
PBCB6	363.5	0.95	1.36	4.63
mesogen including oxygen	194.2	1	2.22	3.76
PBCB6 spacer no mesogen	142.2	0.9	0.472	5.51
backbone	27.0	0.9	0.415	5.57
95% D5CB	267.5	1.08	5.98	0

scattering length density around the axis of the cylinder. We follow a procedure similar to that used by Rawiso et al.[36] to model the scattering from the mesogenic groups. Here we treat the polymer as a three-component particle (consisting of a backbone, a mesogenic unit, and spacer) and calculate the scattering length densities (δ) of the components as

$$\delta = \frac{\rho N_A \sum_k b_k}{M} \tag{6}$$

where N_A is Avogadro's number, M is the component molar mass, ρ is the component density, and b_k is the scattering length density of the kth atom. The contribution of the different components to the total scattering is related to the contrast ($K = \delta_{D5CB} - \delta$) in their scattering length densities according to

$$I_{total}(q) = K_B^2 I_B(q) + K_M^2 I_M(q) + K_S^2 I_S(q) + 2K_B K_M I_{BM}(q) + 2K_B K_S I_{BS}(q) + 2K_S K_M I_{SM}(q) \tag{7}$$

The subscripts B, M, and S refer to the backbone, mesogen, and spacer, respectively, and BM, BS, and SM refer to cross-terms. The calculated values of K and δ are listed in Table 3 along with the estimates of the component densities used for the calculations. Relative to D5CB, the scattering contrast in the spacer and the backbone, $K_S = 5.51$ and $K_B = 5.57$, are somewhat greater than the mesogenic unit, $K_M = 3.76$. Furthermore, the component $I(q)$ values are related to the component sizes, which makes the contributions from the backbone less significant and the spacer and mesogenic unit contributions more significant.

4b. Theoretical Effect of Spacer on the Measured Anisotropy. A theoretical prediction of the effect of a labeled mesogen on the SANS pattern is worked out in Appendix 1, yielding

$$R_{||}^2 = R_{||b}^2 + \frac{L^2(2S+1)}{9} \tag{8}$$

and

$$R_\perp^2 = R_{\perp b}^2 + \frac{L^2(1-S)}{9} \tag{9}$$

Here the effect of the mesogenic units on the measured scattering is shown to be dependent on the order parameter S and on the length of the mesogen, L. In the nematic liquid crystal 5CB, an order parameter of ~0.57 is found at temperatures of ~25 °C.[40] Our refractive index measurements[27] indicate that the order parameter was not significantly changed by the addition of polymer; therefore, $S = 0.57$ can be assumed for our solutions. Equations 8 and 9 indicate that the change in the measured radius due to the mesogenic groups is greater in the parallel direction than in the perpendicular direction. Also, since the effects of the mesogen add to the square of the radius of the backbone, this change will be greater for smaller radii or for lower molecular weights. Therefore, when the mesogenic units are accounted for in an oblate polymer, a greater difference between the anisotropy of the backbone ($R_{\perp b}/R_{||b}$) as compared to the whole molecule ($R_\perp/R_{||}$) is seen for lower molecular weight polymers than for higher molecular weights.

Using the software package MacSpartan, approximate values of 20, 22, and 23 Å were obtained for the length of the mesogenic unit in the polymers PBCB4, PBCB6, and PBCB7, respectively. Using these, along with $S = 0.57$, values for the backbone radii of the polymers were obtained using eqs 8 and 9 (Table 1). Once this effect is taken into account, so that one is considering the conformation of the backbone without the mesogenic units, the polymer anisotropy is $R_{\perp b}/R_{||b} \approx 1.66 \pm 0.05$ for all the polymers. Since eqs 8 and 9 were derived in such a way that the actual topology of the backbone is not taken into account, these equations could also be used to account for the mesogenic contributions to the scattering from branched or star polymers. Therefore, if one assumes that the reactions forming cross-links between polymer chains are similar for the different molecular weights, then the constant anisotropy of $R_{\perp b}/R_{||b} \approx 1.66 \pm 0.05$ for this PBCBx series of polymers is expected.

In our thermal studies of these polymers,[27] we found that in the melt state there was only a weak odd−even effect with spacer length for the enthalpy of the isotropic to nematic transition. We typically observed slow trends toward stronger nematic order and higher transition temperatures as the spacer length was increased. Therefore, the solution properties of this polymer series would not be expected to have significant odd−even effects either. The polymers PBCB4, PBCB5, PBCB7, and PBCB8 are made from the same 63 kg/mol 1,2-polybutadiene prepolymer as the 420 kg/mol PBCB6 polymer. Since all these polymers have the same degree of polymerization and are expected to have only weak trends in the measured radii as the length of the spacer is increased, it is not surprising that they all have a similar anisotropy of $R_{\perp b}/R_{||b} \approx 1.60 \pm 0.07$. The deviations of the measured backbone anisotropies from the average value are primarily due to experimental uncertainty with some variability caused by intermolecular cross-links and an accompanying increase in polydispersity.

Table 4. Literature Data Adjusted for Side-Group Deuteration[a]

DP	temp (°C)	phase	$R_\perp$ (Å)	$R_\parallel$ (Å)	$R_\perp/R_\parallel$	$R_{\perp b}$ (Å)	$R_{\parallel b}$ (Å)	$R_{\perp b}/R_{\parallel b}$
35[b]	60	S	14.6 ± 3	19.2 ± 3	0.76	14.1	10.3	1.37
35[b]	88	N	14.4 ± 3	19.6 ± 3	0.74	13.0	13.0	1.00
80[b]	56	S	41.2 ± 3	25.7 ± 3	1.61	41.1	19.9	2.06
80[c]	85	N			1.12 ± 0.1[d]			1.13 ± 0.1[e]
80[b]	95	N	27.0 ± 3	28.5 ± 3	0.95	26.3	24.5	1.07

[a] Data points for the polymer with a DP of 80 at temperatures of 70 and 82 °C were omitted because they both did not fit the trends for a transition between a nematic and a smectic phase and they had large inconsistencies with the measurements by Noirez et al.[24] at 85 °C. [b] Hardouin et al.[21] and Pepy et al.[23] data. [c] Noirez et al.[24] data. [d] In Noirez et al.[24] the numerical value of the anisotropy was not given in the text; it was estimated by noting that the scattered intensity is a function of $I(qR_x)$. Therefore, by estimating the ratio of the slopes in Figure 12 of Noirez et al.,[24] an estimation of the anisotropy was obtained similar to Casquilho and Volino.[25] [e] This estimate was obtained by assuming a value for $R_\perp = 27$ Å.

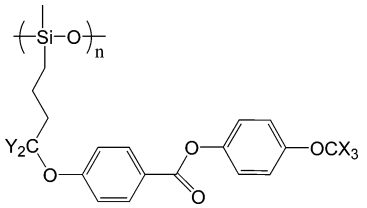

Figure 7. Polymer used by Hardouin et al.,[21] Moussa et al.,[22] and Pepy et al.[23] with (X = D, Y = H) and by Noirez et al.[24] with (X = H, Y = D).

The absence of trends with spacer length is analogous to the results of Gu et al.[41] when studying the effects of spacer length on the director relaxation rate for a series of SGLCPs dissolved in 5CB. They found that for either very small or very large spacer lengths the effect on the relaxation rate was the greatest, but for intermediate lengths there was no dependence on spacer lengths. This is similar to our system in that we are also at an intermediate spacer length where the mesogens are sufficiently decoupled from the backbone to have only negligible differences in their effect on the backbone anisotropy.

4c. Comparison with Prior Literature on SGLCP Melts. We have applied this method of accounting for the effects of scattering from side groups in SGLCPs to the melt studies of other researchers and will demonstrate how it explains inconsistencies in their measured anisotropy. Using a poly(methylsiloxane) where different parts of the side group were selectively deuterated (Figure 7), Hardouin et al.,[21] Moussa et al.,[22] Pepy et al.,[23] and Noirez et al.[24] found some dependence of the polymer anisotropy on molecular weight and on the location of the deuterium label. For the sample with DP = 35, in both the nematic and smectic phases the polymer conformation was prolate with equal anisotropies of $R_\perp/R_\parallel \approx 0.75$. This is unexpected for two reasons. First, in smectic SGLCPs the polymer backbone is primarily located in the space between the layers with infrequent crossings resulting in the backbone taking on an oblate conformation.[39] Second, in end-on SGLCPs the anisotropy of the nematic phase is usually lower than in the smectic phase.

When Hardouin et al.[21] and Pepy et al.[23] used a polymer with DP=80, the effects of the side group were less important and more typical results were obtained. They measured an anisotropy of $R_\perp/R_\parallel \approx 1.61$ and $R_\perp/R_\parallel \approx 0.95$ in the smectic and nematic phases, respectively. This anisotropy for the smectic phase is small, but still reasonable, and a transition from an oblate to a prolate conformation is possible but unusual.[42]

The same reasoning applied to the PBCBx system was applied to this siloxane based system in Appendix 2, yielding

$$R_\parallel^2 = R_{\parallel b}^2 + \frac{l^2(2S+1)}{3} \tag{10}$$

and

$$R_\perp^2 = R_{\perp b}^2 + \frac{l^2(1-S)}{3} \tag{11}$$

An estimated value for the smectic order parameter, $S_S = 0.85$, was obtained by comparison with a polymethacrylate[43] SGLCP with a similar structure at approximately 12 °C below its smectic to nematic transition temperature (T_{sn}). The nematic order parameter $S_n = 0.6$ was estimated as the average value found by Demange et al.[44] using a polymethacrylate SGLCP. Labeling distances of $l = 17$ and $l = 4$, from Casquilho and Volino,[25] corresponding to labeling on the terminal methoxy group and the spacer group, respectively, were used.

After the application of these values using eqs 10 and 11, more reasonable values for the anisotropy of the backbone were obtained (Table 4). In the smectic phase the anisotropy is $R_{\perp b}/R_{\parallel b} = 1.37$ and 2.06 for a DP = 35 and 80, respectively. These two values are not equal as one might expect, but this could be due to one of two reasons. First of all, the uncertainty in the measurements of the radii is ±3 Å, which, especially for the small polymer, could result in a large uncertainty. Second, the polymer may be too small to approach a steady-state high molecular weight value for the anisotropy. This second explanation fits well with the observations of Shibaev et al.,[39] using polymethacrylates with a similar mesogenic group, that in the smectic phase the anisotropy increased with molar mass and that the steady-state anisotropy was not reached until molar masses greater than 100 kg/mol were approached.

In the nematic phase the anisotropy is $R_{\perp b}/R_{\parallel b} = 1.00$ and 1.07 for DP = 35 and 80, respectively, when the polymer is labeled on the terminal methoxy group. When the labeling is on the spacer group, a more reliable anisotropy is measured, $R_{\perp b}/R_{\parallel b} = 1.13$, where the effects of the labeling position only change the anisotropy by +0.01. The discrepancy between the anisotropy for terminal vs spacer labeling is most likely due to the ±3 Å variability in the measurements of the radii. This method for accounting for the scattering due to the mesogenic units explains the inconsistencies due to the choice of labeling in this polymer.

5. Conclusions

This study demonstrates a way in which the radii of an SGLCP in a nematic solvent can be measured at low

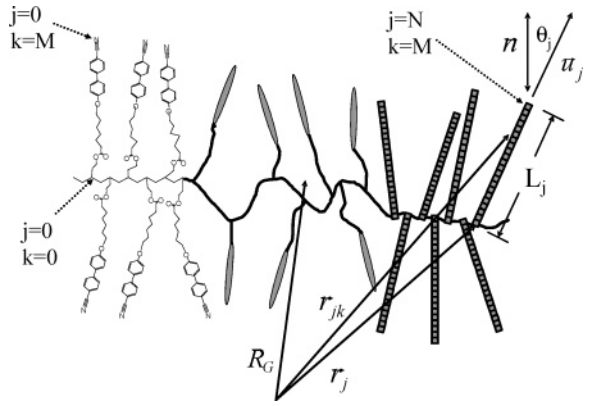

Figure 8. Schematic of PBCB6 showing the definitions of the variables used in the calculations. From left to right the schematic shows different levels of detail: chemical structure, schematic structure, and the mathematical structure used for this study.

concentration while maintaining adequate scattering intensity. In melt studies, a 50:50 mixture of polymer with deuterium labeling on the backbone is typically used. For solution studies, concentrations of 5% polymer were used to avoid interchain scattering. If a deuterated solvent is used, the amount of labeling per chain is increased by a factor of 8−10. The effects of these two conditions serve to cancel each other out to give scattering that is comparable with typical 50:50 mixtures. This method could also be used on a 50:50 mixture of perdeuterated and hydrogenated polymer, resulting in greatly increased signal strength.

A polymer analogous synthetic approach enabled us to create a model series of large SGLCPs with narrow molecular weight distributions, matched backbone lengths, and varied side groups. For the spacer lengths from 4 to 8 carbons an oblate conformation was found using SANS with a perdeuterated solvent, D5CB. Using a molecular weight series from DP ≅ 220 to 1150 we show that the overall anisotropy increases with increasing molecular weight for oblate SGLCPs that are long enough to be described as a freely jointed chain. Theories[11,12] have predicted that for low molecular weights the backbone is modeled as a stiff rod but that as the molecular weight increases, the polymer adopts a Gaussian conformation which should result in a backbone anisotropy that is independent of molecular weight. These theories only consider the conformation of the backbone, whereas SANS due to an unlabeled SGLCP in a deuterated solvent measures scattering arising from the entire molecule. By taking into account the contribution of the side groups to the scattering, eqs 8 and 9, the increase in the measured anisotropy can be explained and the radii, $R_{\perp b}$ and $R_{\parallel b}$, can be determined.

This experimental method addresses the need for measurements of the radii of gyration of SGLCPs in nematic solvents to test predicted relationships between chain anisotropy and effects of SGLCP on the Leslie−Ericksen viscosity parameters. Because of the difficulty of measuring the polymer anisotropy in a nematic solution, little work has been done in this area, but by using perdeuterated solvents with SGLCPs, comparison of the Brochard theory with experiments is more easily accomplished.

Acknowledgment. The authors acknowledge financial support from the AFOSR LC-MURI (f4962-97-1-0014) and the ARCS foundation. We thank Neal Scruggs and Rafael Verduzco for help with the neutron scattering experiments and Ed Lang from IPNS for helping with the SANS setup.

Appendix 1. Mathematical Compensation for Side-Group Scattering

In a solution, the radius of gyration of a polymer is typically defined as[45]

$$R_g^2 \equiv \frac{1}{N+1}\left\langle \sum_{j=0}^{N} (\vec{r}_j - \vec{r}_G)^2 \right\rangle \tag{A1}$$

with

$$\vec{r}_G \equiv \frac{1}{N+1}\left\langle \sum_{j=0}^{N} \vec{r}_j \right\rangle \tag{A2}$$

Here $\vec{r}_G$ represents the position vector of the center of gravity of the chain, $\vec{r}_j$ represents the position vector of the jth segment of the polymer backbone, and the brackets indicate a statistical average over all polymer conformations. In a liquid crystalline system, the chain conformation is anisotropic with an axis of symmetry along the director, $\vec{n}$. For studies of SGLCPs in which labeling for neutron scattering contrast is localized on the chain backbone, eq A1 can be rewritten to describe an anisotropic configuration using the quadratic characteristic size of the backbone (R_{xb})

$$R_{xb}^2 \equiv \frac{1}{N+1}\left\langle \sum_{j=0}^{N} (\vec{r}_j \cdot \vec{x} - \vec{r}_G \cdot \vec{x})^2 \right\rangle \tag{A3}$$

where $\vec{x}$ is a unit vector in an arbitrary direction. Here we take the further step of accounting for scattering from pendant groups on an SGLCP. We model each monomeric unit as a set of M equal scatterers, instead of a single scatterer on the backbone (Figure 8). This is accomplished by changing the summation in eq A3 to include scattering from each of M scatterers in the pendant group:

$$R_x^2 \equiv \frac{1}{N+1}\left\langle \sum_{j=0}^{N} \frac{1}{M} \sum_{k=0}^{M} (\vec{r}_{jk} \cdot \vec{x} - \vec{r}_G \cdot \vec{x})^2 \right\rangle \tag{A4}$$

Here, $\vec{r}_{jk}$ is the position vector of the kth scatterer on the jth side group, and R_x is the quadratic characteristic size in the $\vec{x}$ direction, including the effects of the bulky side group as observed by neutron scattering. If the jth side group is described as having an orientation unit vector $\vec{u}_j$ with an effective length L_j and if one assumes the scatterers are spaced evenly and contribute equally to the total intensity, then

$$\vec{r}_{jk} = \vec{r}_j + \frac{kL_j\vec{u}_j}{M} \tag{A5}$$

and

$$R_x^2 \equiv \frac{1}{N+1}\left\langle \sum_{j=0}^{N} \frac{1}{M} \sum_{k=0}^{M} \left(\vec{r}_j \cdot \vec{x} + \frac{kL_j\vec{u}_j}{M} \cdot \vec{x} - \vec{r}_G \cdot \vec{x} \right)^2 \right\rangle \tag{A6}$$

In the limit as M becomes large, the side group can be modeled as a uniform distribution of scattering length density instead of as discrete scatterers, and the sum-

mation can be approximated as an integral

$$R_x^2 \equiv \frac{1}{N+1}\left\langle \sum_{j=0}^{N} \frac{1}{L_j}\int_0^{L_j} (\vec{r}_j\cdot\vec{x} + y\vec{u}_j\cdot\vec{x} - \vec{r}_G\cdot\vec{x})^2 \mathrm{d}y \right\rangle \quad \text{(A7)}$$

where $y = kL_j/M$. This assumption is valid since, as shown earlier, the scattering contrast of the different components are similar. Within this mathematical framework, the greater scattering density contrast of the spacer relative to the mesogen will cause the effective length L_j to be slightly smaller in SANS experiments. This factor is small enough so that the uncertainty in measurement should be greater than the uncertainty due to this approximation.

Integrating eq A7 and noting that because of the symmetry of a nematic LC

$$\frac{1}{N+1}\left\langle \sum_{j=0}^{N} L_j\vec{u}_j\cdot\vec{x}(\vec{r}_j - \vec{r}_G)\cdot\vec{x} \right\rangle = 0 \quad \text{(A8)}$$

yields

$$R_x^2 \equiv \frac{1}{N+1}\left\langle \sum_{j=0}^{N} \left[(\vec{r}_j\cdot\vec{x} - \vec{r}_G\cdot\vec{x})^2 + \frac{(L_j\vec{u}_j\cdot\vec{x})}{3} \right] \right\rangle \quad \text{(A9)}$$

The first term in this equation equals the characteristic size of the polymer backbone, eq A3. Here we use the subscript "b" to emphasize the fact that this term represents the radius one would measure if only the backbone was labeled

$$R_x^2 = R_{xb}^2 + \left\langle \frac{(L_j\vec{u}_j\cdot\vec{x})^2}{3} \right\rangle \quad \text{(A10)}$$

The second term in eq A10 represents the average, over the length of the polymer chains, of the squared extension of the side group in the $\vec{x}$ direction. In uniaxial liquid crystals the order parameter, S, is defined by

$$S = \frac{1}{2}\langle 3\cos^2\theta_j - 1\rangle \quad \text{(A11)}$$

Here θ_j is the angle of an individual mesogen relative to the director and, in our case, a mesogenic side group of the SGLCP. If one assumes that the order parameter takes variations in the effective mesogen length and orientation into account, then

$$\langle (L_j\vec{u}_j\cdot\vec{x})^2\rangle = L^2\langle\cos^2\theta\rangle \quad \text{(A12)}$$

when $\vec{x}$ is parallel to the director and

$$\langle (L_j\vec{u}_j\cdot\vec{x})^2\rangle = \frac{1}{2}L^2\langle\sin^2\theta\rangle \quad \text{(A13)}$$

when $\vec{x}$ is perpendicular to the director. The factor of $^1/_2$ is present in eq A13 since there are two orthogonal axes perpendicular to the director and the squares of the projections of the director on the three axes must add up to 1. In terms of the order parameter and the ensemble averaged length of the side group, L, eq A10 yields eqs 8 and 9.

Appendix 2. Mathematical Compensation for Scattering from a Single Labeled Site

The same reasoning applied to the PBCBx system can be applied to this siloxane-based system by modifying eq A4 to approximate the scattering from the polymer as a single scatterer located at a position $\vec{u}\vec{x}l_j$ from the backbone of each chain segment.

$$R_x^2 \equiv \frac{1}{N+1}\left\langle \sum_{j=0}^{N} (\vec{r}_j\cdot\vec{x} + l_j\vec{u}_j\cdot\vec{x} - \vec{r}_G\cdot\vec{x})^2 \right\rangle \quad \text{(A14)}$$

In an analogous approach, a similar result to eq A10 is found

$$R_x^2 = R_{xb}^2 + \langle (l_j\vec{u}_j\cdot\vec{x})^2\rangle \quad \text{(A15)}$$

At this point, we have produced nearly the same equation to account for the labeling as Noirez et al.[24] They, however, did not take into account the order parameter. This allowed them to demonstrate qualitative agreement between the measured anisotropy and their model. To obtain quantitative agreement between the model and the data, we take into account the order parameter, eq A11, as before and obtain eqs 10 and 11. Hardouin et al.,[21] Moussa et al.,[22] and Pepy et al.[23] used the Guinier approximation, eq 2, to calculate the quadratic characteristic size. This equation is derived for any arbitrary set of scatterers, in the range where $qR_x < 1$, and can be applied to eqs 10 and 11 without any further assumptions.

References and Notes

(1) Brochard, F. *J. Polym. Sci., Polym. Phys.* **1979**, *17*, 1867.
(2) Mattoussi, H.; Veyssie, M.; Casagrande, C.; Guedeau, M. A. *Mol. Cryst. Liq. Cryst.* **1987**, *144*, 211.
(3) Jamieson, A. M.; Gu, D.; Chen, F. L.; Smith, S. *Prog. Polym. Sci.* **1996**, *21*, 981.
(4) Liu, P. Y.; Yao, N.; Jamieson, A. M. *Macromolecules* **1999**, *32*, 6587.
(5) Chiang, Y. C.; Jamieson, A. M.; Zhao, Y.; Kasko, A. M.; Pugh, C. *Polymer* **2002**, *43*, 4887.
(6) Chiang, Y. C.; Jamieson, A. M.; Campbell, S.; Tong, T. H.; Sidocky, N. D.; Chien, L. C.; Kawasumi, M.; Percec, V. *Polymer* **2000**, *41*, 4127.
(7) Yao, N.; Jamieson, A. M. *Macromolecules* **1997**, *30*, 5822.
(8) Kempe, M. D.; Kornfield, J. A. *Phys. Rev. Lett.* **2003**, *90*, 115501.
(9) Mattoussi, H. *Mol. Cryst. Liq. Cryst.* **1990**, *178*, 65.
(10) Mattoussi, H.; Ober, R.; Veyssie, M.; Finkelmann, H. *Europhys. Lett.* **1986**, *2*, 233.
(11) Wang, X. J.; Warner, M. *J. Phys. A: Math. Gen.* **1987**, *20*, 713.
(12) Maffetone, P. L.; Marrucci, G. *J. Rheol.* **1992**, *36*, 1547.
(13) Williams, D. R. M.; Halpern, A. *Macromolecules* **1993**, *26*, 2025.
(14) Carri, G. A.; Muthukumar, M. *J. Chem. Phys.* **1998**, *109*, 11117.
(15) D'Allest, F. F.; Maissa, P.; Bosch, A. T.; Sixou, P. *Phys. Rev. Lett.* **1988**, *61*, 2562.
(16) Mattoussi, H.; Ober, R. *Macromolecules* **1990**, *23*, 1809.
(17) Cherodian, A. S.; Hughes, N. J.; Richardson, R. M.; Lee, M. S. K.; Gray, G. W. *Liq. Cryst.* **1993**, *14*, 1667.
(18) Noriez, L.; Pepy, G. *Phys. Scr.* **1988**, *T25*, 102.
(19) Kirste, R. G.; Ohm, H. G. *Makromol. Chem., Rapid Commun.* **1985**, *6*, 179.
(20) Pepy, G.; Cotton, J. P.; Hardouin, F.; Keller, P.; Lambert, M.; Moussa, F.; Noirez, L.; Lapp, A.; Strazielle, C. *Makrolmol. Chem., Macromol. Symp.* **1988**, *15*, 251.
(21) Hardouin, F.; Noirez, L.; Keller, P.; Lambert, M. Moussa, F.; Pepy, G. *Mol. Cryst. Liq. Cryst.* **1988**, *155*, 389.
(22) Moussa, F.; Cotton, J. P.; Hardouin, F.; Keller, P.; Lambert, M.; Pepy, G.; Mauzac, M.; Richard, H. *J. Phys. (Paris)* **1987**, *48*, 1079.
(23) Pepy, G.; Noirez, L.; Keller, P.; Lambert, M.; Moussa, F.; Cotton, J. P.; Strazielle, C.; Lapp, A. Hardouin, F.; Mauzac, M.; Richard, H. *Makromol. Chem.* **1990**, *191*, 1383.
(24) Noirez, L.; Keller, P.; Cotton, J. P. *Liq. Cryst.* **1995**, *18*, 129.
(25) Casquilho, J. P.; Volino, F. *Mol. Cryst. Liq. Cryst.* **1990**, *180B*, 357.

(26) Kempe, M. D.; Auad, M. L.; Kornfield, J. A.; Wu, S. T.; Zhou, W. J. Manuscript in preparation.
(27) Kempe, M. D.; Kornfield, J. A.; Ober, C. K.; Smith, S *Macromolecules* **2004**, *37*, 3569.
(28) E7 and E44 are cyanobiphenyl-based eutectic mixtures composed primarily of the liquid crystals 5CB and 5OCB.
(29) Wu, S. T.; Wang, Q. H.; Kempe, M. D.; Kornfield, J. A. *J. Appl. Phys.* **2002**, *92*, 7146.
(30) Cotton, J. P.; Hardouin, F. *Prog. Polym. Sci.* **1997**, *22*, 795.
(31) Carri, G. A.; Muthukumar, M. *J. Chem. Phys.* **1998**, *109*, 11117.
(32) Higgins, J. S.; Benoit, H. C. *Polymers and Neutron Scattering*; Oxford University Press: Oxford, 1996.
(33) Keller, P.; Carvalho, B.; Cotton, J. P.; Lambert, M.; Moussa, F.; Pepy, G. *J. Phys., Lett.* **1985**, *46*, L-1065.
(34) Noirez, L.; Boeffel, C.; Aladine, A. D. *Phys. Rev. Lett.* **1998**, *80*, 1453.
(35) Kunchenko, A. B.; Svetogorsky, D. A. *Liq. Cryst.* **1987**, *2*, 617.
(36) Rawiso, M.; Duplessix, R.; Picot, C. *Macromolecules* **1987**, *20*, 630.
(37) Richardson, R. M.; Gray, G. W.; Tajbakhsh, A. R. *Liq. Cryst.* **1993**, *14*, 871.
(38) O'Allest, J. F.; Sixou, P.; Blumstein, A.; Blumstein, R. B.; Teixeira, J.; Noirez, L. *Mol. Cryst. Liq. Cryst.* **1988**, *155*, 581.
(39) Shibaev, V. P.; Barmatov, E. B.; Yongjiee, T.; Richardson, R. *Polym. Sci.* **2000**, *42*, 1680.
(40) Guo, W.; Fung, B. M. *J. Chem. Phys.* **1991**, *95*, 3917.
(41) Gu, D. F.; Smith, S. R.; Jamieson, A. M.; Lee, M.; Percec, V. *J. Phys. II* **1993**, *3*, 937.
(42) Noirez, L.; Keller, P.; Davidson, P.; Hardouin, F.; Cotton, J. P. *J. Phys. (Paris)* **1988**, *49*, 1993.
(43) Wittmann, J. C.; Meyer, S.; Damman, P.; Dosiere, M.; Schmidt, H.-W. *Polymer* **1998**, *39*, 3545.
(44) Demange, V. F.; Boue, F.; Brulet, A.; Keller, P.; Cotton, J. P. *Macromolecules* **1998**, *31*, 801.
(45) Cloizeaux, J. D.; Janink, G. *Polymers in Solution*; Clarendon Press: Oxford, 1990.

MA034825F